Ag@TiO$_2$ Nanocomposite as an Efficient Catalyst for Knoevenagel Condensation

Mostafa Sayed,* Zhipeng Shi, Farzad Gholami, Pedram Fatehi,* and Ahmed I. A. Soliman*

Cite This: *ACS Omega* 2022, 7, 32393−32400

Read Online

ACCESS | Metrics & More | Article Recommendations | Supporting Information

ABSTRACT: In the present study, a new series of different heterocycles was synthesized through base-free Knoevenagel condensation of various aldehydes and active methylene-containing compounds using the hydrothermal developed Ag@TiO$_2$ as a heterogeneous catalyst. The catalyst was synthesized by mixing TiO$_2$ (P25) with AgNO$_3$ and hydrothermally treated in ethanol at 180 °C for 12 h. The developed Ag@TiO$_2$ catalyst was directly applied for Knoevenagel condensation, and the optimized procedure involved stirring the aldehydes and active methylene-containing compounds with Ag@TiO$_2$ in ethanol at 65 °C. The reaction scope was investigated for various aromatic and heterocyclic aldehydes with active methylene-containing compounds, and the isolated yields were significantly high. The reusability of the catalyst was investigated for up to five cycles, where an insignificant decrease in the catalyst's reactivity was observed. Also, the reaction could proceed in water as a solvent, and the isolated yield was 40%. Hence, this protocol features mild reaction conditions, a facile procedure, and clean reaction profiles.
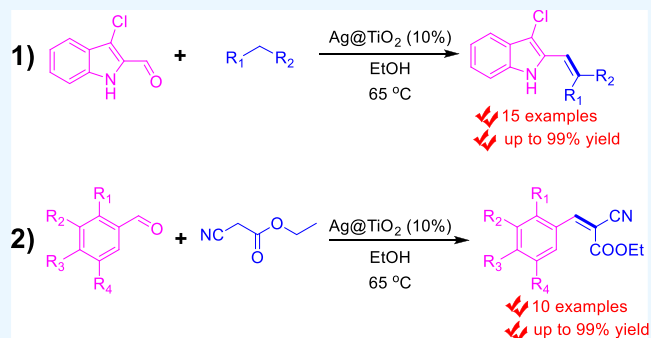
1. INTRODUCTION

Knoevenagel condensation is a reaction involving nucleophilic addition of a hydrogen active species to a carbonyl compound generally aldehyde or ketone followed by dehydration, resulting in olefin compounds, and this reaction commonly occurs in the presence of a weakly basic amine catalyst.[1−3] This reaction has originally been described by the German chemist Emil Knoevenagel, and it can be described as a modification of the aldol condensation.[4] The importance of this reaction originated from its feasibility route for the synthesis of various biologically active compounds containing C═C bonds.[3] The α,β-unsaturated products produced from the Knoevenagel reaction had mostly been used as potential intermediates in the synthesis of many naturally occurring compounds,[5] therapeutic agents,[6,7] adequate chemicals,[8] and polymers containing different functional groups.[9]

As mentioned above, the Knoevenagel reaction is common in academics and industry, with broad applications in pharmaceutical synthesis.[7,10] Usually, the reaction is homogeneously catalyzed by organic bases such as piperidine, and this convention method suffers from many difficulties like time-consuming work-up procedures, undesired side products, applying high temperatures, difficult catalyst isolation, and hazardous reaction residues.[11] Because of these limitations, many efforts have been devoted in this area to find alternative routes to perform this reaction under base-free conditions. Previous studies have reported the use of different heterogeneous catalysts containing zeolites, mesoporous silica, ionic liquids, and graphitic carbon nitride.[12,13] Also, composites containing metal oxides showed high reactivity as heterogeneous catalysts for Knoevenagel condensation, and the metal oxides in these composites were prior chemically modified or doped with metals.[14−17]

Titanium dioxide (TiO$_2$)-based catalysts are considered promising and recyclable catalysts for organic synthesis, and metal or nonmetal dopants would enhance the catalytic stability and activity.[18] Noble metal-doped TiO$_2$ catalysts are widely used for the synthesis of Schiff bases,[19] reduction of nitrobenzenes to hydrazobenzens,[20] and dehydrogenation of *n*-heterocycles.[21] One of these promising catalysts is Ag@TiO$_2$, which is used as an effective catalyst in the synthesis of bis(pyrazol-5-ol) and dihydropyrano[2,3-*c*]pyrazole, pyrido-[2,3-*d*]pyrimidine, benzimidazole, and benzoxazole derivatives.[22−25] For the Knoevenagel condensation, composites of TiO$_2$-La$_2$O$_2$CO$_3$, Fe$_3$O$_4$@SiO$_2$@TiO$_2$, and mesoporous TiO$_2$−CeO$_2$ were reported to be effective catalysts.[15,26,27]

Inspired by these studies, Ag@TiO$_2$ was utilized in this study as the catalyst for the reactions between 3-chloro-1*H*-

indole-2-carbaldehydes and other aromatic aldehydes with different compounds containing active methylene. Indole-containing compounds represent an important class of heterocyclic compounds because of their use as alkaloid precursors,[28] and their biological activities, such as anti-tumor,[29] antiviral,[30] and anti-inflammatory activity.[31] Besides, the 3-chloro-1*H*-indole-2-carbaldehyde is an easily accessible source for indole carbaldehyde, which can be functionalized at the 2-position to produce various heterocyclic compounds with the chlorine atom at the 3-position, which may boost their biological activities.[32−36] Reaction optimization and detailed scope are comprehensively studied. Also, the recyclability of the catalyst is investigated, and the reaction mechanism is suggested. Such a comprehensive study of Knoevenagel condensation on Ag@TiO$_2$ has not been previously reported to the best of our knowledge. Successful completion of Knoevenagel condensation using such recyclable Ag@TiO$_2$ catalyst without applying other hazardous homogenous catalysts would pave the way for a facile, green, and environmental-friendly synthetic method of heterocyclic compounds.

2. EXPERIMENTAL SECTION

2.1. Synthesis of Ag@TiO$_2$. One gram of TiO$_2$ (P25, Degussa, 20 nm, the Brunauer−Emmett−Teller (BET) surface area is 50 ± 15 m^2/g), 20 mL of water, and 20 mL of ethanol were transferred into a Teflon vessel. After that, a Teflon container was sonicated in an ultrasonic cleaning bath (40 kHz) and magnetically stirred for 20 min each. The calculated amounts of AgNO$_3$ (Sigma, ≥99%) were added into the Teflon container, sonicated, and stirred for 20 min for homogenous mixing with TiO$_2$ to prepare Ag(5%)@TiO$_2$. After that, the Teflon container was sealed and transferred into a hydrothermal synthesis autoclave reactor and heated at 180 °C for 12 h. After completing the hydrothermal process, the reactor was left to be cooled down in an ambient environment, and the Ag@TiO$_2$ was separated using a centrifuge at 4000 rpm. The product was washed three times using deionized water and dried at 60 °C for 24 h.

2.2. General Method for Knoevenagel Condensation. 3-Chloro-1*H*-indole-2-carbaldehyde (**1a**, 0.5 g, 3 mmol) was introduced into a 50 mL reaction vessel with ethyl cyanoacetate (0.41 g, 3.9 mmol), 20 mL of solvent, and the developed catalyst (50 mg). The resulting mixture was warmed and stirred at 60 °C in an oil bath for 1 h. Ethyl acetate (20 mL) was added to the reaction mixture after TLC confirmed that the reaction had been completed. The catalyst was then filtered out of the mixture. Under reduced pressure, the solvent was evaporated, disclosing the desired final product.

2.3. Characterization Instruments. The XRD measurements of the developed catalysts were investigated by A Philips 1700 version diffractometer with Cu Kα radiation. The morphology and crystallinity of the developed catalyst were examined by TEM (JEOL, JEM-2100F, Japan), where an accelerating voltage of 200 kV was applied. Also, the element mapping was investigated by applying energy-dispersive X-ray spectroscopy (EDX). The XPS analysis was performed using a Kratos Axis Supra spectrometer with a monochromatic Al Kα radiation (1486.7 eV) at low pressure (<10$^{−6}$ Pa). The collected spectra were analyzed by CasaXPS software. The BET method was applied to estimate the surface area and average pore size of Ag@TiO$_2$ samples using NOVA 2200e (Quantachrome Instruments). The degasification was per-

formed prior to the measurements under vacuum at 100 °C for 12 h. Fourier transform infrared (FTIR) spectra of the developed catalysts were collected using a Bruker Tensor 37 spectrometer, where an ATR accessory was used with 4 cm$^{−1}$ resolution. NMR spectra were collected using an INOVA-500 MHz instrument (Varian, Palo Alto, CA, USA), and trimethylsilyl propanoic acid (TSP) was used as an internal standard.
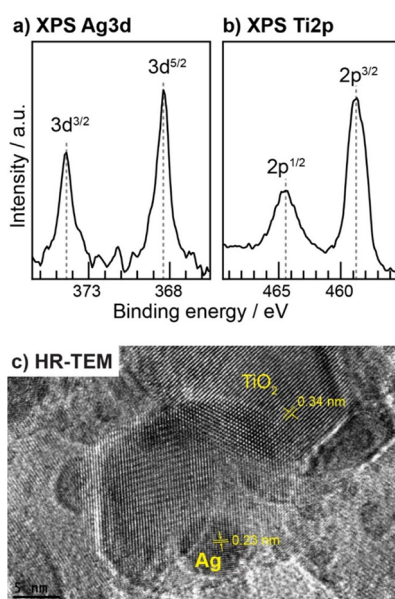
3. RESULTS AND DISCUSSION

3.1. Catalyst Characterization. Figure 1a shows the TiO$_2$ (P25) XRD patterns before and after Ag loading. At 27.3°,
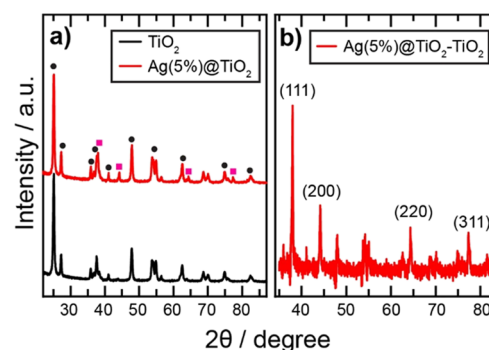
Figure 1. XRD spectra of (a) TiO$_2$, Ag@TiO$_2$, and (b) Ag@TiO$_2$ after subtracting the TiO$_2$ spectrum.

35.9°, 41.1°, 54.9°, 56.5°, 68.9°, and 70.0°, characteristic peaks were observed and indexed to (110), (101), (111), (211), (220), (301), and (112) crystallographic rutile TiO$_2$ planes, respectively.[19,37,38] The characteristic peaks at 25.1°, 37.6°, 47.8°, 53.7°, 62.7°, 75.0°, and 82.5° were indexed to (101), (004), (200), (105), (204), (215), and (303) crystallographic anatase TiO$_2$ planes, respectively.[19,38,39] After the hydro-thermal process in the presence of AgNO$_3$, new characteristic peaks at 44.2°, 64.3°, and 77.3° were observed in Figure 1a, which were indexed to the (200), (220), and (311) planes of Ag nanoparticles, respectively.[40−42] Figure 1b shows the XRD spectra of normalized Ag(5%)@TiO$_2$ after subtracting the normalized XRD spectrum of TiO$_2$ to resolve the overlapping between the characteristic peaks of Ag and TiO$_2$. A characteristic peak at 2θ of 38° was observed, which is indexed to the (111) crystallographic planes of Ag nanoparticles.[41,42] Peaks attributed to the (200), (220), and (311) crystallo-graphic planes of Ag were also found at the same position. These XRD data illustrated that the Ag(0) was successfully formed on TiO$_2$ without changing the phases of TiO$_2$.[40−42]

Figure 2a shows the XPS Ag3d spectrum, where two peaks were observed at 368.4 and 374.4 eV, which are attributed to 3d$^{5/2}$ and 3d$^{3/2}$, respectively. The energy separation between the two peaks is 6 eV, which illustrates the reduction of Ag$^+$ to metallic Ag nanoparticles.[40−42] The XRD spectrum of Ti2p is shown in Figure 2b, where two peaks corresponding to 2p$^{3/2}$ and 2p$^{1/2}$ were observed at 458.8 and 464.5 eV.[40,42] The separation between the two peaks is 5.7 eV which is the characteristic of Ti^{+4} of TiO$_2$. Figure S1 shows the TEM image after the hydrothermal deposition of Ag nanoparticles on TiO$_2$, where the sizes of Ag and TiO$_2$ nanoparticles were almost <10 nm and >20 nm, respectively. Besides, Ag nanoparticles with a size of <5 nm were observed and well distributed. Figure 2c shows the high resolution (HR)TEM image, where the $d_{spacing}$
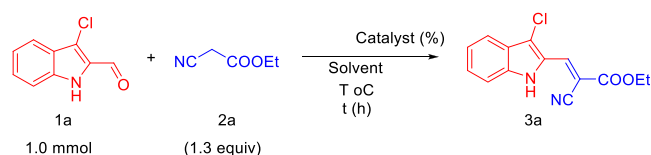
Figure 2. (a) XPS Ag3d spectrum, (b) XPS Ti2p spectrum, and (c) HR-TEM of Ag(5%)@TiO$_2$.

Table 1. Optimization of Reaction Conditions[a]

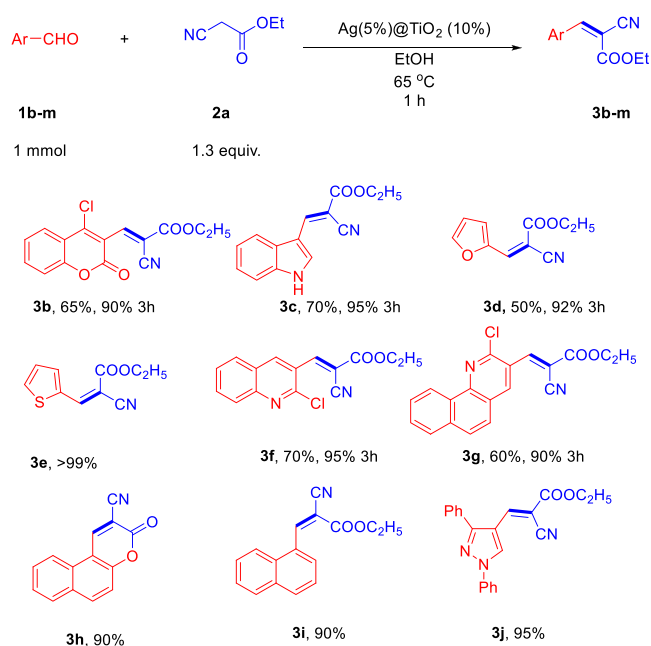| entry	catalyst	catalyst load (mg)	solvent	T (°C)	t (h)	yield (%)[b]
1		10	EtOH	65	1	
2	TiO$_2$	10	EtOH	65	1	10
3	Au(5%)@TiO$_2$	10	EtOH	65	1	70
4	Pt(5%)@TiO$_2$	10	EtOH	65	1	50
5	Ag(5%)@TiO$_2$	10	EtOH	65	1	90
6	Ag(1%)@TiO$_2$	10	EtOH	65	1	60
7	Ag(3%)@TiO$_2$	10	EtOH	65	1	65
8	Ag(5%)@TiO$_2$	10	H$_2$O	65	1	40
9	Ag(5%)@TiO$_2$	10	CH$_2$Cl$_2$	65	1	traces
10	Ag(5%)@TiO$_2$	10	CH$_3$CN	65	1	22
11	Ag(5%)@TiO$_2$	0.5	EtOH	65	1	traces
12	Ag(5%)@TiO$_2$	5	EtOH	65	1	30
13	Ag(5%)@TiO$_2$	15	EtOH	65	1	68
14	Ag(5%)@TiO$_2$	20	EtOH	65	1	70
15	Ag(5%)@TiO$_2$	10	EtOH	30	1	45
16	Ag(5%)@TiO$_2$	10	EtOH	50	1	50
17	Ag(5%)@TiO$_2$	10	EtOH	60	1	63
18	Ag(5%)@TiO$_2$	10	EtOH	65	0.5	50
19	Ag(5%)@TiO$_2$	10	EtOH	65	2	90

[a]Reaction conditions: **1a** (1.0 mmol), **2a** (1.3 equiv), catalyst (0.005 mmol), ethanol (15 mL). [b]Isolated yield.

of 0.23 and 0.34 nm were attributed to the $d_{spacing}$ of Ag (111) and anatase TiO$_2$ (101), respectively.[19,42] The polycrystallinity of Ag@TiO$_2$ due to the presence of Ag, anatase TiO$_2$, and rutile TiO$_2$ nanoparticles was also indicated from the SAED image illustrated in Figure S2. The EDX mapping of TiO$_2$ and Ag(5%)@TiO$_2$ components is illustrated in Figure S3, where the distribution of titanium, oxygen, and silver elements is shown. The BET surface area of TiO$_2$ (P25) increased to 78 m^2/g after 5% Ag doping, which indicates the increase in the catalyst reactivity after doping.

3.2. Knoevenagel Condensation. *3.2.1. Optimal Reaction Conditions.* As previously stated, 3-chloro-1*H*-indole-2-carbaldehyde (**1a**) represents an easily accessible source for the synthesis of 3-chloro-2-substituted indoles, so compound **1a** was selected as a model substrate for this transformation, which then was allowed to react with ethyl cyanoacetate as the active hydrogen-containing compound, as illustrated in Table 1. Carrying out the reaction in the absence of the catalyst gave no product at all. However, the addition of TiO$_2$ (P25) nanoparticles to the reaction slightly enhanced the reaction activity, and product **3a** was separated in a 10% yield (entry 2). Following the optimal conditions that we have previously obtained for the synthesis of Schiff bases using Au (5%)@TiO$_2$,[19] we successfully isolated the Knoevenagel product in a 70% yield (entry 3). The use of the Pt@TiO$_2$ catalyst gave a 50% yield product (entry 4). It has been reported that higher loadings of Au or Pt on TiO$_2$ would reduce the catalytic activity because of the increase in the sizes of the nanoparticles leading to a decrease in the active sites.[43,44] Interestingly, the Ag (5%)@TiO$_2$ catalyst smoothly delivered the product in a 90% yield as the best reaction yield (entry 5). Moreover, trying different Ag doping amounts on TiO$_2$ represented in 1% and 3% successfully delivered the product, but the yields were 60% and 65%, respectively (entries 6 and 7). Previous studies showed that the Ag loadings on TiO$_2$ with up to 10% would increase the adsorption capacity and photocatalytic activities of TiO$_2$.[45,46] In Figure S1, the Ag nanoparticles with <5 nm were also observed and well distributed on TiO$_2$, which could illustrate the reactivity increase with increasing Ag loadings.

Furthermore, optimization using different solvents (entries 8−10) suggested that ethanol is the optimal solvent. Besides, increasing the catalyst load to 15 or 20 mg did not result in high yields, but when the load was attenuated to 0.5 or 5 mg, it led to the diminishing of the isolated yield (entries 11−14). Reaction time and temperature were finally screened showing that the product smoothly obtained in a good yield when the reaction was conducted at 65 °C for 1 h (entries 15−19).

3.2.2. Reaction Scope. After identifying the optimal reaction conditions, the scope of this transformation using different aldehydes and active methylene-containing compounds was investigated. The target of this study is to find an eco-friendly approach for synthesizing different heterocyclic moieties through Knoevenagel condensation because of their biological importance. Hence, we turned our attention to the screening of different heterocyclic carbaldehydes, as shown in Table 2. The reaction proceeded smoothly with a wide range of heterocyclic aldehydes providing an interesting class of *α,β*-unsaturated heterocycles. Both monocyclic and fused heterocyclic aldehydes were tolerated in this transformation under the optimal conditions. Aldehydes containing thiophene and pyrazole moieties gave the products **3e**, **3j** with an excellent yield up to 99%, while furan-2-carbaldehyde gave the product **3d** in only 50% yield after 1 h; however, for a prolonged time of 3 h, **3d** was isolated in 90% yield. Thiophene is well known to be adsorbed on noble metals like Au or Ag, which might facilitate the condensation and enhance the isolated yield.[47,48] Fused heterocyclic aldehydes underwent the reaction smoothly to afford Knoevenagel derivatives in good yields (up to 95%), where coumarin, quinoline, and naphthalene-containing carbaldehydes have fascinatedly tolerated in this conversion

Table 2. Substrate Scope of Aldehydes

3b, 65%, 90% 3h   **3c**, 70%, 95% 3h   **3d**, 50%, 92% 3h

3e, >99%   **3f**, 70%, 95% 3h   **3g**, 60%, 90% 3h

3h, 90%   **3i**, 90%   **3j**, 95%

with acceptable yields. Notably, tricyclic benzoquinoline aldehyde **1g** underwent Knoevenagel condensation to give the product **3g** in a 90% yield after 3 h. Interestingly, the reaction of 2-hydroxy-1-naphthaldehyde (**1h**) with ethyl cyanoacetate under the optimal conditions led to the formation of 3-oxo-3H-benzo[*f*]chromene-2-carbonitrile (**3h**) instead of *α,β*-unsaturated product, which resulted from the cyclic condensation of the Knoevenagel intermediate by loss of the ethanol molecule, which has been further assigned by mass spectroscopy.

The scope of active methylene-containing compounds with 3-chloro-1*H*-indole-2-carbaldehyde was also examined under the standard reaction conditions, as shown in Table 3; various active methylene derivatives were found to be suitable substrates in this transformation with a good yield (between 80 and 99%). The use of cyanoacetamide and cyanothioacetamide produced derivatives **3m** and **3o** in 85 and 80%, respectively, while malononitrile and acetylacetone gave the **3k** and **3n** products in 82 and 99% yields, respectively. Moreover,

Table 3. Substrate Scope of Active Methylene-Containing Compounds

3k, 82 %   **3l**, 98%   **3m**, 85 %

3n, > 99 %   **3o**, 80%   **3p**, 85%
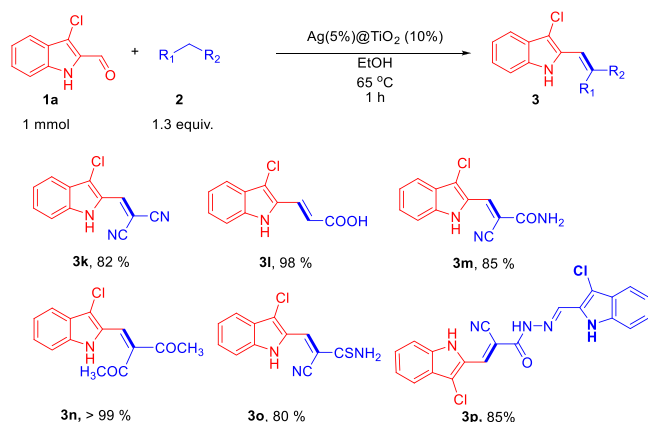
the condensation of aldehyde **1a** with malonic acid under the standard conditions gave the acrylic acid derivative **3l** in 98%, which resulted from the decarboxylation of the Knoevenagel intermediate.[32] Furthermore, the substrates of indole-bearing active hydrogen were compatible enough in this methodology, producing **3p** in 85%.

The generality of the current catalytic system has also extended to include different aromatic aldehydes that make the catalytic system more effective, as shown in Table 4. To

Table 4. Substrate Scope of Aromatic Aldehydes and Ethyl Cyanoacetate

3na, 95%   **3oa**, 95%   **3pa**, 98%

3qa, 95%   **3ra**, 94%   **3sa**, 96%

3ta, 95%   **3ua**, 97%   **3va**, 98%

3wa, 99%
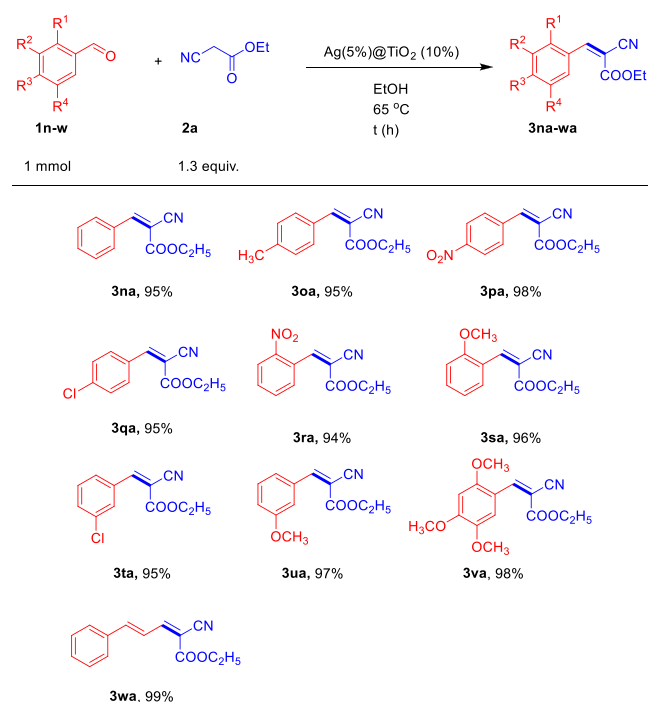
product	yield (%)	time (min)	lit. m.p. (°C)	obtained m.p. (°C)
3na	95	30	47−48[49]	48−49
3oa	95	45	89−91[50]	90−91
3pa	98	30	168[50]	166−167
3qa	95	30	89−90[51]	84−85
3ra	94	60	97−98[52]	97−99
3sa	95	60	70−72[49]	72−73
3ta	95	60	160−161[51]	158−160
3ua	97	30	53−54[53]	55−56
3va	98	30		152−153
3wa	99	30	112−114[54]	113−115

achieve this goal, benzaldehyde was allowed to react with ethyl cyanoacetate under the standard conditions, and the product **3na** was delivered in a 95% yield. Moreover, different aromatic aldehydes with electron-donating or electron-withdrawing substituents in o-, p-, and m-positions have been examined. *p*-Tolualdehyde reacted smoothly to give the product **3oa** in 95% yield, whereas benzaldehyde with an electron deficiency NO_2 group in the *p*-position exhibited more activity, and the product **3pa** separated in 98% yield. Also, *p*-chlorobenzaldehyde has successfully reacted to produce the product **3qa** in a 95%yield. Furthermore, different aromatic aldehydes with *o*-substituents, namely, *o*-nitrobenzaldehyde and *o*-anisaldehyde have been examined, and the **3ra** and **3sa** products were isolated in 94 and 95%, respectively. Moreover, *m*-substituted

benzaldehyde including *m*-chlorobenzaldehyde and *m*-anisal-dehyde have also successfully checked in this reaction, which gave products **3ta** and **3ua** in 95 and 97% yields, respectively. Finally, more substituted 2,4,5-trimethoxy benzaldehyde and cinnamaldehyde have also been tolerated, which afforded the products **3va** and **3wa** in excellent yields.

To show the synthetic utility of the Ag(5%)@TiO₂, the yield of the **3na** product and the applied procedures of some catalysts that have been reported are listed in Table 5. The present protocol offers advantages in the isolated yields, reaction time, and reaction conditions compared to the other catalysts.

Table 5. Comparison of Ag@TiO₂-Catalyzed Knoevenagel Condensation of 1n with 2a for the Yields of 3na Product with Other Heterogeneous Catalysts

entry	catalyst	time (min)	conditions	yield (%)	ref.
1	Ag@TiO₂	60	EtOH, 65 °C	95	this work
2	MgC₂O₄/SiO₂	1.2	solvent-free, microwave	87	55
3	Pd@g-C₃N₄	180	toluene, 65 °C	88.3	56
4	Ti(IV)@polycarbosilane	7200	ethyl acetate, 50 °C	95	57
2	cobalt hydroxyapatite	5	solvent-free, 80 °C	91	58
3	Al₂O₃-OK	30	EtOH, reflux	98	59
5	Br₃-TBA-Fe₃O₄	60	H₂O, reflux	91	60
6	Alum-Cs₂CO₃	180	H₂O, reflux	94	61
7	Li₂O/ZnO	90	solvent-free, 100 °C	94	62

To explore the synthetic practicality of our designed reaction, a scale-up protocol was carried out by the reaction of benzaldehyde (**1n**) with ethylcyano acetate (**2a**) under the optimal reaction conditions (Figure 3). It proceeded smoothly

to deliver the product **3na** in a 95% yield. Given the versatile reactivity of the Knoevenagel products, in addition, indoles-tethered pyrazole or pyrimidine are considered one of the essential scaffolds in the medicinal chemistry field and found to exhibit a variety of biological activities,[63,64] a variety of further transformations can be carried out to generate new structures. For example, the hydrazinolysis of **3c** in ethanol gave an interesting aminopyrazolidenone derivative **4**.[65] Moreover, the reaction of compound **3c** with thiourea in ethanol delivered the indolyl thioxopyrimidine derivative **5**. Furthermore, the reaction of compound **3c** with urea in ethanol and potassium carbonate gave the Biginelli product dihydropyrimidine **6**.

3.2.3. Reaction Mechanism. According to the above-mentioned findings and based on the previously reported studies concerning Knoevenagel condensation, the suggested mechanism for Ag@TiO₂ catalyzed Knoevenagel condensation is illustrated in Figure 4.[66,67] Among various condensation reactions, Knoevenagel condensation is a well-known reaction, and it can be catalyzed by different kinds of organic bases, acids, or catalysts containing both acid and basic sites.[15,68] The mechanism can be explained as, in the first step, the acidic centers of Ag@TiO₂ would activate the carbonyl group of aldehydes to coordinate between these centers and the oxygen of carbonyl groups.[15,19,24] The active hydrogen species would attach to the carbon of the carbonyl group, which then protonated and underwent water elimination, resulting in the product. The coordination environment surrounding the Ag centers is anticipated to prevent the sterically congested Z-type product.

3.2.4. Recyclability. Catalyst recycling was performed by separating the catalysts from the reaction mixture. Then, the separated catalyst was washed in ethanol three times and dried at 80 °C for 12 h. The recycled catalyst was characterized by FTIR and XRD. The XRD pattern (Figure S4) of the recycled catalyst, where the characteristic peaks of Ag nanoparticles, rutile TiO₂, and anatase TiO₂ were still observed without significant changes compared to the as-prepared Ag@TiO₂
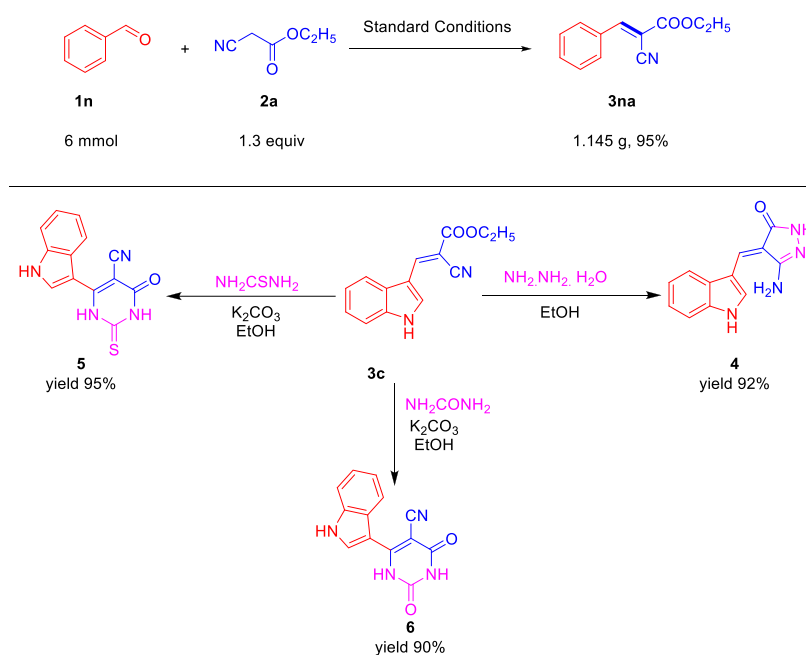

Figure 3. Gram-scale reaction and synthetic applications.
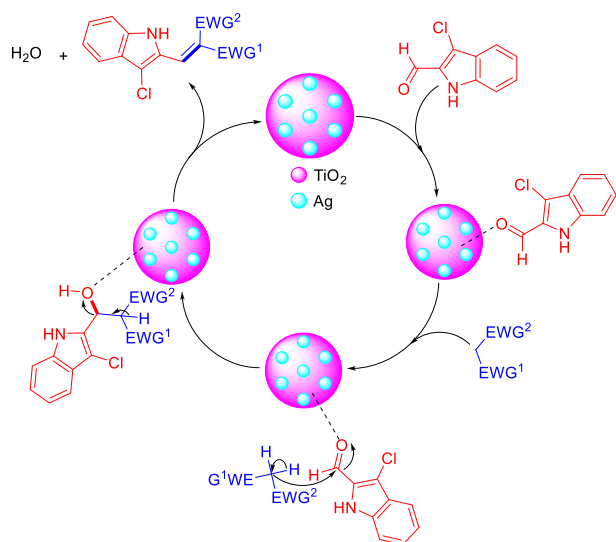
Figure 4. Plausible mechanism for the Ag@TiO$_2$ mediated Knoevenagel condensation reaction.

indicating the stability of the recycled catalyst. The FTIR spectra of the as-prepared and recycled Ag@TiO$_2$ catalyst are illustrated in Figure S5, where the absorption bands at 1400 and <700 cm^{-1} were ascribed to Ti−O−Ti (TiO$_2$).[19,69] Bands at 1615 and 3413 cm^{-1} were attributed to the absorbed water.[19,69] No significant changes were observed after recycling. As previously described, the development of the Ag@TiO$_2$ catalyst is facile without requiring complicated steps or careful handling. Besides, the use of this catalyst for performing Knoevenagel condensation did not require harsh conditions or applying hazardous materials. Also, the catalyst was effective alongside 5 cycles without a significant decrease in the isolated yield, as shown in Figure 5. These results
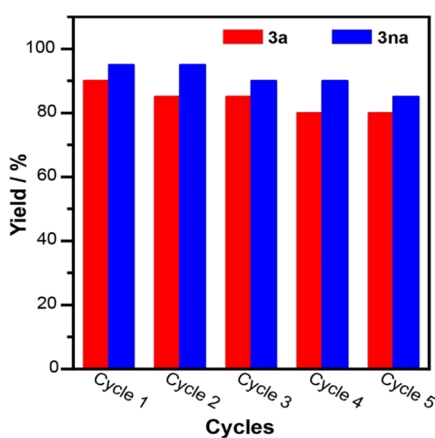
Figure 5. Recyclability of Ag@TiO$_2$ for the synthesis of **3a** and **3na** products.

illustrate the reactivity of Ag@TiO$_2$ in catalyzing the Knoevenagel condensation for several cycles. Also, green, and eco-friendly conditions can be applied during Knoevenagel condensation in the presence of Ag@TiO$_2$, and the yield approaches up to 40%. Besides, the reuse of the catalyst does not require specific treatments.

4. CONCLUSIONS

In conclusion, we developed a new catalytic strategy for Knoevenagel condensation of different carbonyl compounds with various active hydrogen species using the Ag@TiO$_2$ catalyst. The synthesis of Ag@TiO$_2$ was performed through the hydrothermal method. The use of Ag@TiO$_2$ for Knoevenagel condensation enables us to avoid the use of hazardous materials or apply harsh conditions. The presence of Ag@TiO$_2$ activates the carbonyl groups of aldehydes facilitating the interactions with the active methylene-containing compounds. No significant decrease in the catalyst reactivity alongside 5 cycles was observed. Various kinds of carbonyl compounds have been tolerated in this transformation, including aryl and heterocyclic aldehydes. Moreover, a wide spectrum of active methylene-containing compounds has been investigated, showing high isolated yields. Gram-scale protocol and product functionalization have been conducted to explore the utilization of our current designed strategy. Hence, the findings from this study could highlight the use of Ag@TiO$_2$ in Knoevenagel condensation for the synthesis of novel heterocyclic compounds, which is important in the organic synthesis discipline.

■ ASSOCIATED CONTENT

Ⓢ Supporting Information

The Supporting Information is available free of charge at https://pubs.acs.org/doi/10.1021/acsomega.2c03852.

> TEM, SAED, EDX mapping, XRD, FTIR, and analytical data of Knoevenagel products (color, melting point, IR, ^{1}H-NMR, ^{13}C-NMR, and MS) (PDF)

■ AUTHOR INFORMATION

Corresponding Authors

Mostafa Sayed − *Department of Chemistry, University of Science and Technology of China, Hefei 230026, China; Chemistry Department, Faculty of Science, New Valley University, El-Kharja 72511, Egypt;* ⓞ orcid.org/0000-0002-5469-0129; Email: mostafaali@mail.ustc.edu.cn, mostafasayed@sci.nvu.edu.eg

Pedram Fatehi − *Chemical Engineering Department, Lakehead University, Thunder Bay, ON P7B5E1, Canada;* ⓞ orcid.org/0000-0002-3874-5089; Email: pfatehi@lakeheadu.ca

Ahmed I. A. Soliman − *Chemical Engineering Department, Lakehead University, Thunder Bay, ON P7B5E1, Canada; Chemistry Department, Faculty of Science, Assiut University, Assiut 71516, Egypt;* ⓞ orcid.org/0000-0001-8851-3887; Email: ahmed.soliman.38z@science.aun.edu.eg

Authors

Zhipeng Shi − *Department of Chemistry, University of Science and Technology of China, Hefei 230026, China*

Farzad Gholami − *Chemical Engineering Department, Lakehead University, Thunder Bay, ON P7B5E1, Canada*

Complete contact information is available at:
https://pubs.acs.org/10.1021/acsomega.2c03852

Notes

The authors declare no competing financial interest.

■ REFERENCES

(1) Tietze, L. F. Domino Reactions in Organic Synthesis. *Chem. Rev.* **1996**, *96*, 115−136.

(2) Freeman, F. Properties and Reactions of Ylidenemalononitriles. *Chem. Rev.* **1980**, *80*, 329−350.

(3) Khare, R.; Pandey, J.; Smriti, S.; Ruchi, R. The Importance and Applications of Knoevenagel Reaction (Brief Review). *Orient. J. Chem.* **2019**, *35*, 423−429.

(4) List, B. Emil Knoevenagel and the Roots of Aminocatalysis. *Angew. Chem., Int. Ed.* **2010**, *49*, 1730−1734.

(5) Heravi, M. M.; Janati, F.; Zadsirjan, V. Applications of Knoevenagel Condensation Reaction in the Total Synthesis of Natural Products. *Monatsh. Chem.* **2020**, *151*, 439−482.

(6) Kraus, G. A.; Krolski, M. E. Synthesis of a Precursor to Quassimarin. *J. Org. Chem.* **1986**, *51*, 3347−3350.

(7) Tokala, R.; Bora, D.; Shankaraiah, N. Contribution of Knoevenagel Condensation Products toward the Development of Anticancer Agents: An Updated Review. *ChemMedChem* **2022**, *17*, No. e2021007.

(8) Zahouily, M.; Salah, M.; Bahlaouane, B.; Rayadh, A.; Houmam, A.; Hamed, E. A.; Sebti, S. Solid Catalysts for the Production of Fine Chemicals: The Use of Natural Phosphate Alone and Doped Base Catalysts for the Synthesis of Unsaturated Arylsulfones. *Tetrahedron* **2004**, *60*, 1631−1635.

(9) Liang, F.; Pu, Y. J.; Kurata, T.; Kido, J.; Nishide, H. Synthesis and Electroluminescent Property of Poly(p-Phenylenevinylene)s Bearing Triarylamine Pendants. *Polymer* **2005**, *46*, 3767−3775.

(10) Madivada, L. R.; Anumala, R. R.; Gilla, G.; Alla, S.; Charagondla, K.; Kagga, M.; Bhattacharya, A.; Bandichhor, R. An Improved Process for Pioglitazone and Its Pharmaceutically Acceptable Salt. *Org. Process Res. Dev.* **2009**, *13*, 1190−1194.

(11) Tietze, L. F.; Beifuss, U. The Knoevenagel Reaction. *Compr. Org. Synth.* **1991**, *1*, 341−394.

(12) Appaturi, J. N.; Ratti, R.; Phoon, B. L.; Batagarawa, S. M.; Din, I. U.; Selvaraj, M.; Ramalingam, R. J. A Review of the Recent Progress on Heterogeneous Catalysts for Knoevenagel Condensation. *Dalton. Trans.* **2021**, *50*, 4445−4469.

(13) Liang, J.; Liang, Z.; Zou, R.; Zhao, Y. Heterogeneous Catalysis in Zeolites, Mesoporous Silica, and Metal-Organic Frameworks. *Adv. Mater.* **2017**, *29*, No. 1701139.

(14) Yuan, X.; Wang, J.; Wan, Z.; Zhang, Q.; Luo, J. One-Pot Suzuki Coupling-Knoevenagel Condensation Tandem Reaction Catalyzed by a Recyclable Magnetic Bifunctional Catalyst. *ChemistrySelect* **2021**, *6*, 1238−1243.

(15) Wang, F.; Hu, K.; Bi, Y.; Wei, X.; Xue, B. Knoevenagel Condensation Reaction on a New Highly-Efficient La$_2$O$_2$CO$_3$-TiO$_2$ Mixed Oxide Catalyst: Composition-Effects on C=C Bond Formation. *Chem. Phys.* **2020**, *539*, No. 110942.

(16) Göksu, H.; Gültekin, E. Pd Nanoparticles Incarcerated in Aluminium Oxy-Hydroxide: An Efficient and Recyclable Heterogeneous Catalyst for Selective Knoevenagel Condensation. *ChemistrySelect* **2017**, *2*, 458−463.

(17) Wang, G.; Ding, Z.; Meng, L.; Yan, G.; Chen, Z.; Hu, J. Magnetically Recoverable 2-(Aminomethyl)Phenols-Modified Nanoparticles as a Catalyst for Knoevenagel Condensation and Carrier for Palladium to Catalytic Suzuki Coupling Reactions. *Appl. Organomet. Chem.* **2020**, *34*, 1−12.

(18) Oi, L. E.; Choo, M. Y.; Lee, H. V.; Ong, H. C.; Hamid, S. B. A.; Juan, J. C. Recent Advances of Titanium Dioxide (TiO$_2$) for Green Organic Synthesis. *RSC Adv.* **2016**, *6*, 108741−108754.

(19) Soliman, A. I. A.; Sayed, M.; Elshanawany, M. M.; Younis, O.; Ahmed, M.; Kamal El-Dean, A. M.; Abdel-Wahab, A.-M. A.; Wachtveitl, J.; Braun, M.; Fatehi, P.; Tolba, M. S. Base-Free Synthesis and Photophysical Properties of New Schiff Bases Containing Indole Moiety. *ACS Omega* **2022**, 10178−10186.

(20) Liu, Q.; Zhang, J.; Xing, F.; Cheng, C.; Wu, Y.; Huang, C. Applied Surface Science Plasmon-Enhanced and Controllable Synthesis of Azobenzene and Hydrazobenzene Using Au/TiO$_2$ Composite. *Appl. Surf. Sci.* **2020**, *500*, No. 144214.

(21) Balayeva, N. O.; Mamiyev, Z.; Dillert, R.; Zheng, N.; Bahnemann, D. W. Rh/TiO$_2$-Photocatalyzed Acceptorless Dehydrogenation of N-Heterocycles upon Visible-Light Illumination. *ACS Catal.* **2020**, *10*, 5542−5553.

(22) Maleki, B.; Baghayeri, M.; Vahdat, S. M.; Mohammadzadeh, A.; Akhoondi, S. Ag@TiO$_2$ Nanocomposite; Synthesis, Characterization and Its Application as a Novel and Recyclable Catalyst for the One-Pot Synthesis of Benzoxazole Derivatives in Aqueous Media. *RSC Adv.* **2015**, *5*, 46545−46551.

(23) Bhardwaj, D.; Dhawan, K.; Singh, R. On Water Greener Synthesis of Pyrido[2,3-d]Pyrimidines Using Ag-TiO$_2$ Nanocomposite Catalyst under Sonication. *J. Iran. Chem. Soc.* **2022**, *19*, 1003−1013.

(24) Fatahpour, M.; Noori Sadeh, F.; Hazeri, N.; Maghsoodlou, M. T.; Hadavi, M. S.; Mahnaei, S. Ag/TiO$_2$ Nano-Thin Films as Robust Heterogeneous Catalyst for One-Pot, Multi-Component Synthesis of Bis (Pyrazol-5-Ol) and Dihydropyrano[2,3-c]Pyrazole Analogs. *J. Saudi Chem. Soc.* **2017**, *21*, 998−1006.

(25) Tang, L.; Guo, X.; Yang, Y.; Zha, Z.; Wang, Z. Gold Nanoparticles Supported on Titanium Dioxide: An Efficient Catalyst for Highly Selective Synthesis of Benzoxazoles and Benzimidazoles. *Chem. Commun.* **2014**, *50*, 6145−6148.

(26) Khazaei, A.; Gholami, F.; Khakyzadeh, V.; Moosavi-Zare, A. R.; Afsar, J. Magnetic Core-Shell Titanium Dioxide Nanoparticles as an Efficient Catalyst for Domino Knoevenagel-Michael-Cyclocondensation Reaction of Malononitrile, Various Aldehydes and Dimedone. *RSC Adv.* **2015**, *5*, 14305−14310.

(27) Mohammed, M. S.; Bakhtiarian, M.; Bahrami, K. Mesoporous Titania−Ceria Mixed Oxide (MTCMO): A Highly Efficient and Reusable Heterogeneous Nanocatalyst for One-Pot Synthesis of β-Phosphonomalonates via a Cascade Knoevenagel−Phospha-Michael Addition Reaction. *J. Exp. Nanosci.* **2020**, *15*, 54−69.

(28) Mizoguchi, H.; Oikawa, H.; Oguri, H. Biogenetically Inspired Synthesis and Skeletal Diversification of Indole Alkaloids. *Nat. Chem.* **2014**, *6*, 57−64.

(29) Ma, J.; Li, J.; Guo, P.; Liao, X.; Cheng, H. Synthesis and Antitumor Activity of Novel Indole Derivatives Containing α-Aminophosphonate Moieties. *Arab. J. Chem.* **2021**, *14*, No. 103256.

(30) Dorababu, A. Indole-a Promising Pharmacophore in Recent Antiviral Drug Discovery. *RSC Med. Chem.* **2020**, *11*, 1335−1353.

(31) Pan, G.; Zhao, Y.; Ren, S.; Liu, F.; Xu, Q.; Pan, W.; Yang, T.; Yang, M.; Zhang, X.; Peng, C.; Hao, G.; Kong, F.; Zhou, L.; Xiao, N. Indole-Terpenoids With Anti-Inflammatory Activities From Penicillium Sp. HFF16 Associated With the Rhizosphere Soil of *Cynanchum Bungei* Decne. *Front. Microbiol.* **2021**, *12*, No. 710364.

(32) Sayed, M.; El-dean, A. M. K.; Ahmed, M.; Hassanien, R.; Sayed, M.; El-dean, A. M. K.; Ahmed, M.; Hassanien, R. Synthesis of Some Heterocyclic Compounds Derived from Indole as Antimicrobial Agents. *Synth. Commun.* **2018**, *48*, 413−421.

(33) Sayed, M.; Kamal El-Dean, A. M.; Ahmed, M.; Hassanien, R. Synthesis, Characterization, and Screening for Anti-Inflammatory and Antimicrobial Activity of Novel Indolyl Chalcone Derivatives. *J. Heterocycl. Chem.* **2018**, *55*, 1166−1175.

(34) Sayed, M.; Younis, O.; Hassanien, R.; Ahmed, M.; Mohammed, A. A. K.; Kamal, A. M.; Tsutsumi, O. Design and Synthesis of Novel Indole Derivatives with Aggregation-Induced Emission and Antimicrobial Activity. *J. Photochem. Photobiol., A* **2019**, *383*, No. 111969.

(35) Sayed, M.; Kamal El-Dean, A. M.; Ahmed, M.; Hassanien, R. Design, Synthesis, and Characterization of Novel Pyrimidines Bearing Indole as Antimicrobial Agents. *J. Chin. Chem. Soc.* **2019**, *66*, 218−225.

(36) Tolba, M. S.; Sayed, M.; Kamal El-dean, A. M.; Hassanien, R.; Ahmed, M.; Abdel-Raheem, S. A. A. Design, Synthesis and Antimicrobial Screening of Some New Thienopyrimidines. *Org. Commun.* **2021**, *4*, 365−376.

(37) Almashhori, K.; Ali, T. T.; Saeed, A.; Alwafi, R.; Aly, M.; Al-Hazmi, F. E. Antibacterial and Photocatalytic Activities of Controllable (Anatase/Rutile) Mixed Phase TiO$_2$ Nanophotocatalysts Synthesized: Via a Microwave-Assisted Sol-Gel Method. *New J. Chem.* **2020**, *44*, 562−570.

(38) Linley, S.; Liu, Y.; Ptacek, C. J.; Blowes, D. W.; Gu, F. X. Recyclable Graphene Oxide-Supported Titanium Dioxide Photocatalysts with Tunable Properties. *ACS Appl. Mater. Interfaces* **2014**, *6*, 4658−4668.

(39) Abazari, R.; Mahjoub, A. R.; Sanati, S. A Facile and Efficient Preparation of Anatase Titania Nanoparticles in Micelle Nanoreactors: Morphology, Structure, and Their High Photocatalytic Activity under UV Light Illumination. *RSC Adv.* **2014**, *4*, 56406−56414.

(40) Liu, G.; Lu, Z.; Zhu, X.; Du, X.; Hu, J.; Chang, S.; Li, X.; Liu, Y. Facile In-Situ Growth of Ag/TiO$_2$ Nanoparticles on Polydopamine Modified Bamboo with Excellent Mildew-Proofing. *Sci. Rep.* **2019**, *9*, 16496.

(41) Zhang, X.; Sun, H.; Tan, S.; Gao, J.; Fu, Y.; Liu, Z. Hydrothermal Synthesis of Ag Nanoparticles on the Nanocellulose and Their Antibacterial Study. *Inorg. Chem. Commun.* **2019**, *2019*, 44−50.

(42) Zhang, L.; Lu, H.; Chu, J.; Ma, J.; Fan, Y.; Wang, Z.; Ni, Y. Lignin-Directed Control of Silver Nanoparticles with Tunable Size in Porous Lignocellulose Hydrogels and Their Application in Catalytic Reduction. *ACS Sustainable Chem. Eng.* **2020**, *8*, 12655−12663.

(43) Murdoch, M.; Waterhouse, G. I. N.; Nadeem, M. A.; Metson, J. B.; Keane, M. A.; Howe, R. F.; Llorca, J.; Idriss, H. The Effect of Gold Loading and Particle Size on Photocatalytic Hydrogen Production from Ethanol over Au/TiO$_2$ Nanoparticles. *Nat. Chem.* **2011**, *3*, 489−492.

(44) Dong, W.; Reichenberger, S.; Chu, S.; Weide, P.; Ruland, H.; Barcikowski, S.; Wagener, P.; Muhler, M. The Effect of the Au Loading on the Liquid-Phase Aerobic Oxidation of Ethanol over Au/TiO$_2$ Catalysts Prepared by Pulsed Laser Ablation. *J. Catal.* **2015**, *330*, 497−506.

(45) Sirivallop, A.; Areerob, T.; Chiarakorn, S. Enhanced Visible Light Photocatalytic Activity of N and Ag Doped and Co-Doped TiO$_2$ Synthesized by Using an In-Situ Solvothermal Method for Gas Phase Ammonia Removal. *Catalysts* **2020**, *10*, 251.

(46) Kılıç, A.; Alev, O.; Özdemir, O.; Arslan, L. Ç.; Büyükköse, S.; Öztürk, Z. Z. The Effect of Ag Loading on Gas Sensor Properties of TiO$_2$ Nanorods. *Thin Solid Films* **2021**, *726*, No. 138662.

(47) Gadogbe, M.; Ansar, S. M.; Chu, I.-W.; Zou, S.; Zhang, D. Comparative Study of the Self-Assembly of Gold and Silver Nanoparticles onto Thiophene Oil. *Langmuir* **2014**, *30*, 11520−11527.

(48) Nambu, A.; Kondoh, H.; Nakai, I.; Amemiya, K.; Ohta, T. Film Growth and X-Ray Induced Chemical Reactions of Thiophene Adsorbed on Au(1 1 1). *Surf. Sci.* **2003**, *530*, 101−110.

(49) Li, G.; Xiao, J.; Zhang, W. Efficient and Reusable Amine-Functionalized Polyacrylonitrile Fiber Catalysts for Knoevenagel Condensation in Water. *Green Chem.* **2012**, *14*, 2234−2242.

(50) Muralidhar, L.; Girija, C. R. Simple and Practical Procedure for Knoevenagel Condensation under Solvent-Free Conditions. *J. Saudi Chem. Soc.* **2014**, *18*, 541−544.

(51) Elhamifar, D.; Kazempoor, S.; Karimi, B. Amine-Functionalized Ionic Liquid-Based Mesoporous Organosilica as a Highly Efficient Nanocatalyst for the Knoevenagel Condensation. *Catal. Sci. Technol.* **2016**, *6*, 4318−4326.

(52) Jayalakshmi, L. N.; Karuppasamy, A.; Stalindurai, K.; Sivaramakarthikeyan, R.; Devadoss, V.; Ramalingan, C. A Mechanochemical Approach for the Construction of Carbon-Carbon Double Bonds: Efficient Syntheses of Aryl/Heteroaryl/Aliphatic Acrylates and Nitriles. *Catal. Lett.* **2015**, *145*, 1322−1330.

(53) Liu, S.; Ni, Y.; Yang, J.; Hu, H.; Ying, A.; Xu, S. Nano-Fe$_3$O$_4$ Encapsulated-Silica Particles Bearing 3-Aminopropyl Group as a Magnetically Separable Catalyst for Efficient Knoevenagel Condensation of Aromatic Aldehydes with Active Methylene Compounds. *Chin. J. Chem.* **2014**, *32*, 343−348.

(54) Gupta, M.; Gupta, R.; Anand, M. Hydroxyapatite Supported Caesium Carbonate as a New Recyclable Solid Base Catalyst for the Knoevenagel Condensation in Water. *Beilstein J. Org. Chem.* **2009**, *5*, 1−7.

(55) Yuan, S.; Li, Z.; Xu, L. Knoevenagel Condensation of Aldehydes with Active Methylene Compounds Catalyzed by MgC$_2$O$_4$/SiO$_2$ under Microwave Irradiation and Solvent-Free Conditions. *Res. Chem. Intermed.* **2012**, *38*, 393−402.

(56) Wang, H.; Wang, Y.; Guo, Y.; Ren, X.-K.; Wu, L.; Liu, L.; Shi, Z.; Wang, Y. Pd Nanoparticles Confined within Triazine-Based Carbon Nitride NTs: An Efficient Catalyst for Knoevenagel Condensation-Reduction Cascade Reactions. *Catal. Today* **2019**, *2019*, 124−134.

(57) Mangala, K.; Sreekumar, K. Polycarbosilane-Supported Titanium(IV) Catalyst for Knoevenagel Condensation Reaction. *Appl. Organomet. Chem.* **2013**, *27*, 73−78.

(58) Pillai, M. K.; Singh, S.; Jonnalagadda, S. B. Solvent-Free Knoevenagel Condensation over Cobalt Hydroxyapatite. *Synth. Commun.* **2010**, *40*, 3710−3715.

(59) Jin, T.-S.; Guo, J.-J.; Liu, H.-M.; Li, T.-S. Synthesis of Ethyl α-Cyanocinnamates Catalyzed by Al$_2$O$_3$−OK Solid Base. *Synth. Commun.* **2003**, *33*, 783−788.

(60) Shiri, L.; Rahmati, S.; Ramezani Nejad, Z.; Kazemi, M. Synthesis and Characterization of Bromine Source Immobilized on Diethylenetriamine-Functionalized Magnetic Nanoparticles: A Novel, Versatile and Highly Efficient Reusable Catalyst for Organic Synthesis. *Appl. Organomet. Chem.* **2017**, *31*, No. e3687.

(61) Taduri, A. K.; Devi, B. R. Alum-Cs$_2$CO$_3$ as a New Recyclable Solid Base Catalyst for the Efficient Syntheses of Arylidenemalononitriles, Esters and Arylcinnamic Acids in Water. *Asian J. Chem.* **2014**, *26*, 1938−1942.

(62) Sunkara, P.; Masula, K.; Puppala, V.; Bhongiri, Y.; Pasala, V. K.; Basude, M. Highly Active Zinc Oxide-Supported Lithium Oxide Catalyst for Solvent-Free Knoevenagel Condensation. *J. Chem. Sci.* **2021**, *133*, 67.

(63) Karrouchi, K.; Radi, S.; Ramli, Y.; Taoufik, J.; Mabkhot, Y. N.; Al-Aizari, F. A.; Ansar, M. Synthesis and Pharmacological Activities of Pyrazole Derivatives: A Review. *Molecules* **2018**, *23*, 134.

(64) Abadi, A. H.; Eissa, A. A. H.; Hassan, G. S. Synthesis of Novel 1,3,4-Trisubstituted Pyrazole Derivatives and Their Evaluation as Antitumor and Antiangiogenic Agents. *Chem. Pharm. Bull.* **2003**, *51*, 838−844.

(65) Belezheva, V. S.; Erofeev, Y. V.; Yares'ko, N. S.; Balabushevich, A. G.; Suvorov, N. N. Synthesis and Properties of Some Lewis and Brönsted Acids of the Indole Series. *Chem. Heterocycl. Compd.* **1978**, *14*, 1088−1093.

(66) Su, C.; Chen, Z.-C.; Zheng, Q.-G. Organic Reactions in Ionic Liquids: Knoevenagel Condensation Catalyzed by Ethylenediammonium Diacetate. *Synthesis* **2003**, *2003*, 0555−0559.

(67) Gheorghe, A.; Tepaske, M. A.; Tanase, S. Homochiral Metal−Organic Frameworks as Heterogeneous Catalysts. *Inorg. Chem. Front.* **2018**, *5*, 1512−1523.

(68) Choudhary, P.; Sen, A.; Kumar, A.; Dhingra, S.; Nagaraja, C. M.; Krishnan, V. Sulfonic Acid Functionalized Graphitic Carbon Nitride as Solid Acid−Base Bifunctional Catalyst for Knoevenagel Condensation and Multicomponent Tandem Reactions. *Mater. Chem. Front.* **2021**, *5*, 6265−6278.

(69) Kırbıyık, Ç.; Akın Kara, D.; Kara, K.; Büyükçelebi, S.; Yiğit, M. Z.; Can, M.; Kuş, M. Improving the Performance of Inverted Polymer Solar Cells through Modification of Compact TiO$_2$ Layer by Different Boronic Acid Functionalized Self-Assembled Monolayers. *Appl. Surf. Sci.* **2019**, *2019*, 177−184.